Quantitative Precipitation Forecasts Associated with Tropical Cyclones near Taiwan

Guo-Ji Jian

CWB/Forecast Center, Taipei, Taiwan

1. Introduction

Factors for improving typhoon QPF are 1) well-predicted tracks, 2) temporal characterizations of storm intensity, 3) realistic simulations of the storm's inner core structure, 4) proper depictions of convective spiral rainbands, and 5) correctly modeling the effect of orography on precipitating features. In this study, the focus will be to evaluate short-range (0-12-h) forecasts of typhoon rainfall using a high-resolution (9-km grid spacing) MM5 and to study the impact of cloud initialization on model performance. To address the model spin-up problem at the CWB in Taiwan, an advanced and systematic data assimilation system, the Local Analysis and Prediction System (LAPS, McGinley et al. 1991; Albers et al. 1996), is applied to ingest the observational data and initialize the mesoscale model (MM5).

During 2003, an extensive network of four high-quality Doppler radars was established over Taiwan on the north (Wu-Fen-Shan; WSR-88D), south (Ken-Ting; METEOR 1000S), east (Hua-Lien; METEOR 1000S), and west (Chi-Ku; METERO 1000S) coasts. Access to satellite data from the Geostationary Operational Environmental Satellite (GOES-9) at the CWB was greatly improved. Both events provided an excellent opportunity to test the impact of diabatic data assimilation on short-range precipitation forecasts associated with tropical cyclones. Both these additional observational capabilities improve the cloud analysis over what was possible in the earlier work with similar themes (Jian et al. 2003). Furthermore, the established operational LAPS/MM5 system has provided an opportunity to compare parallel assimilation experiments with and without the

LAPS cloud analysis for four 2003 tropical cyclones (Tropical Storms Morakot and Vamco,

Typhoon Dujuan, and Tropical Storm Melor) near Taiwan. Two major objectives of this paper are 1) to evaluate the capability of the hot-start model runs to capture the storm's track, rainbands, and inner core structure and 2) to evaluate the LAPS/MM5 system, especially the short-range (0-12-h) QPF associated with tropical cyclones, by validating the forecasts with observational data from 391 rain gauges in Taiwan.

2. Data, LAPS, and MM5 configuration

The data sources included GOES-9 satellite imagery, post analysis of Doppler radar data, surface observations and soundings as well as ship and buoy data over the western North Pacific basin. Furthermore, aerial reconnaissance with Global Positioning System (GPS) dropwindsondes (Wu et al. 2003) provided by National Taiwan University, was operationally available when tropical cyclones approached Taiwan, such as in the cases of Typhoon Dujuan and Tropical Storm Melor. The profiles of wind, temperature, and humidity from the GPS dropwindsondes were transmitted to the CWB in real time for data assimilation by LAPS.

LAPS consists of wind analysis, temperature, geopotential and cloud analysis from the surface to a pressure level of 50hPa using all available data sources. To initialize a mesoscale model diabatically, the dynamic balance scheme (McGinley and Smart 2001) is a necessary and crucial component. This procedure ensures that momentum and mass fields are consistent with the cloud-analysis derived vertical motions. Further details may be seen in the referenced papers (Albers et al. 1996; McGinley et al. 1991), and as discussed in Jian et al. (2003).

The PSU-NCAR MM5 (version 3.5) was configured in nonhydrostatic mode for short-range forecasting at the CWB. The model domain consists of 153 grid points in the east-west direction and 141 grid points in the north-south direction, centered at 23.58N latitude and 120.91E longitude, with a horizontal resolution of 9-km. The horizontal size and geographic location of this MM5 domain is the same as the LAPS data assimilation domain. A total of 30 unevenly spaced sigma levels were used, of which finest resolution is located near the surface. The model top is set at a constant pressure of 100 hPa.

The LAPS analyzed fields and the 15-km horizontal resolution CWB limited-area model data were applied to provide the initial and boundary conditions, respectively for the model atmosphere.

Daily sea surface temperatures were obtained from the National Centers for Environmental Prediction (NCEP). These data were interpolated to the MM5 model grid using the standard preprocessing programs provided by NCAR. The cloud and precipitation process is represented by the Schultz explicit microphysical parameterization (Schultz 1995). Turbulent fluxes in the planetary boundary layer (PBL) are parameterized utilizing the Hong-Pan PBL scheme (Hong and Pan 1996) used in the NCEP medium-range forecasting (MRF) model. The five-layer soil model of MM5 was applied to predict the heat transfer through the model substrate. Radiative processes in the free atmosphere are parameterized using the Rapid Radiative Transfer Model of Mlawer et al. (1997). Klemp and Durran's (1983) upper radiative boundary condition was availed to help wave energy to pass through the model top.

3. Results

a. Hourly precipitation amounts during 0-6-h forecast

The value of the diabatic technique in the first six hours can be better discerned by comparing the observed and predicted hourly precipitation amounts in Fig. 1, which summarizes 4 tropical storm events against the 391 rain gauge stations over Taiwan. In the cases of Vamco (Fig. 1b), Dujuan (Fig. 1c), and Melor (Fig. 1d), the operational runs (VHOTS, DHOTS, and EHOTS) had more realistic rainfall forecasts, with a substantial improvement in 0-6-h quantitative precipitation compared to the parallel experiments (VNCLD, DNCLD, and ENCLD). In the Morakot case, however, the MHOTS forecast, while capturing the areal distribution better than MNCLD (Figure not shown), did over predict the averaged hourly amounts (Fig. 1a). Clearly, the precipitation predicted in the cold start cases of Morakot (MNCLD), Dujuan (DNCLD), and Melor (ENCLD) were under forecast due to the spin-up problem. In the Vamco case (Fig. 1b), the heavy rainfall amounts were produced by summer thunderstorms during the first six hours. Owing to the rapid decay of the thunderstorm, the observed rainfall rapidly decreased during the period between 0900 and 1200 UTC August. Comparing the rain gauge observations to VHOTS and VNCLD in Fig. 1b, we see that the VHOTS captured the timing of thunderstorm rainfall much better than in VNCLD. The VNCLD needed about 2-3-h to spin-up the model rainfall and once formed, the model thunderstorm persisted beyond the observations resulting in strongly over forecast rainfall amounts during the 3-6-h period.

b. Summary results for all four storms

From the case studies we learned that the diabatic technique shows improvement clearly in some cases and not clearly in others. In this section we will composite all the results into a pair of diagrams for both the 0-6-h and the 6-12-h forecast periods so we can obtain single statistics on which to base our evaluation of the technique. Figure 2 shows ETS and bias scores for precipitation for the 0-6-h period (Fig. 2a) and the 6-12-h period (Fig. 2b) for all four events.

For ETS of forecasts for the 0-6-h period one can see in Fig. 2a that the diabatic (hot start) initialization has a positive impact on forecasts of all precipitation thresholds from 5 mm to 50 mm, relative to the cold start forecasts. In the same diagram plots of biases show that the diabatic technique has a positive but consistent biases for all precipitation thresholds. A model forecast with a consistent bias is easier to use operationally than one with a varying bias. The cold start has a variable bias showing characteristic low biases for small thresholds and large biases for large thresholds. Note that for thresholds of 50 mm the bias was over 2, implying that twice as many stations were forecast to exceed a 50 mm threshold relative to those that actually experienced the event.

A different pattern emerges with the 6-12-h forecasts (Fig. 2b). Here the improvement in the diabatically initialized model runs is not so dramatic. Only thresholds in the 15 to 30mm range saw improvement with the diabatic or hot-start initialization. Below 15 mm and above 30mm, model performance was nearly identical. Yet, both models showed substantially more skill (higher ETS) at all thresholds compared to the 0-6-h forecasts. The bias scores reveal that the diabatic initialization has a consistent positive bias similar to the 0-6-h forecast period. The cold start run indicates a nearly perfect bias of 1 across all thresholds.

The four graphs support some of the findings briefly mentioned in the individual case studies:

1. In the early forecast hours the diabatic technique (including clouds and associated motions) allows for faster spin-up of precipitation relative to the cold start (not including clouds). This shows maximum improvement in ETS scores in the early part of the run. The benefit is clearly most evident in the early forecast hours.
2. After the cold start model has had time to spin up, the benefits of hot start are less evident. As the forecast extends father forward in time the limited area of the model domain becomes more influenced by boundary conditions, and may account for verification of the two runs looking more alike.
3. While the diabatic technique spins up precipitation faster than the cold start, the fact that ETS scores in the 0-6-h are smaller than the 6-12-h indicate that the improved spin-up is not doing a complete job.

A complete spin up should show parity in ETS scores in both the early and late periods. Better parameterization of clouds is warranted including improved estimates of in cloud motions and distribution of microphysical variables. The cloud model used is very simplified for both vertical motions and microphysics estimates.

The LAPS/MM5 system is still undergoing refinement. Efforts are currently underway to clarify the reasons for the poor performance in the eyewall (inner core, Fig. 3) simulation of a typhoon. We propose that 9-km grid resolution is not sufficient to properly model this feature in most cases. The cloud analysis specifies a small percentage of supersaturation in the cloudy domain, which is an adjustable parameter. Tests are needed to assess the sensitivity to the level of supersaturation specified. Recent work on the microphysical package (Schultz, personal communication) includes now, allowance for shallow cumulus processes for subsaturated environments. Experiments designed to evaluate this adjustment in other domains have reduced some of the high bias effects by mitigating "grid-point" storms. Here, "grid point" storms refers to the inability of a 9-km grid (with no convective parameterization) to resolve a precipitating feature that may be 6-20 km in size. Under-resolved explicit convection results in convective storms in the model that are too large and efficient resulting in large rain areas and higher rainfall rates. The results are biases greater than 1 seen in Fig. 2. Another effort is aimed at adding a thermodynamic constraint to the cost function equations of LAPS dynamic balance scheme, which could improve the balanced state and allow the use of radar reflectivity directly, helping to eliminate spurious storms that may be in the initial condition. These and other efforts are ongoing to improve the skill of heavy rainfall prediction.

REFERENCES

Albers, S., J. McGinley, D. Birkenheuer, and J. Smart, 1996: The Local Analysis and Prediction System (LAPS): Analyses of clouds, precipitation, and temperature. *Wea. Forecasting*, **11,** 273-287.

Hong, S. –Y., and H. –L. Pan, 1996: Nonlocal boundary layer vertical diffusion in a medium-range forecast model. *Mon. Wea. Rev.*, **124,** 2322-2339.

Jian, G. -J., S. -L. Shieh, and J. A. McGinley, 2003: Precipitation simulation associated with Typhoon Sinlaku (2002) in Taiwan area using the LAPS diabatic initialization for MM5. *Terr. Atmos. Oceanic Sci.*, **14,** 261-288.

Klemp, J. B., and D. R. Durran, 1983: An upper boundary condition permitting internal gravity wave radiation in numerical mesoscale models. *Mon. Wea. Rev.*, **111,** 430-444.

McGinley, J. A., S. Albers, and P. Stamus, 1991: Validation of a composite convective index as defined by a real-time local analysis system. *Wea. Forecasting*, **6,** 337-356.

———————, and J. R. Smart, 2001: On providing a cloud-balanced initial condition for diabatic initialization. *14th Conf. on Numerical Weather Prediction*, Ft. Lauderdale, Amer. Meteor. Soc., 40-44.

Mlawer, E. J., S. J. Taubman, P. D. Brown, M. J. Iacono, and S. A. Clough, 1997: Radiative transfer for inhomogeneous atmosphere : RRTM, a validated correlated-k model for the longwave. *J. Geophys. Res.*, **102(D14),** 16663-16682.

Schultz, P., 1995: An explicit cloud physics parameterization for operational numerical weather prediction. *Mon. Wea. Rev.*, **123,** 3331-3343.

Wu, C. –C., H. –C. Kuo, P. –H. Lin, T. –C. Yeh, J. –S. Hong, T. –C. Chen, C. –H. Liu, and P. –L. Lin, 2003: Priority Typhoon Research — Dropsonde Observations for Typhoon Surveillance near the TAiwan Region, ROCMS, 44, 1-14.

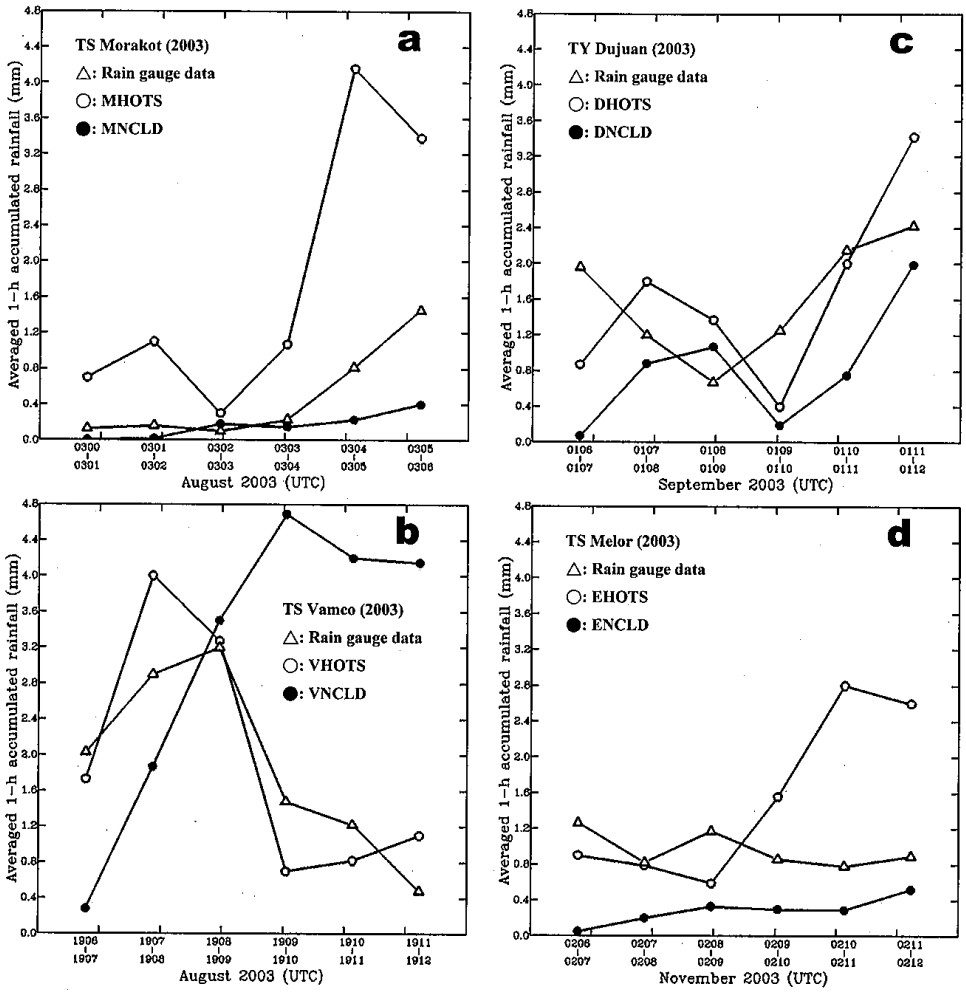

Fig. 1. Hourly accumulated precipitation of (a) Tropical Storm Morakot, (b) Tropical Storm Vamco, (c) Typhoon Dujuan, and (d) Tropical Storm Melor averaged for the 391 rain gauge stations (precipitation verification samples) in Taiwan.

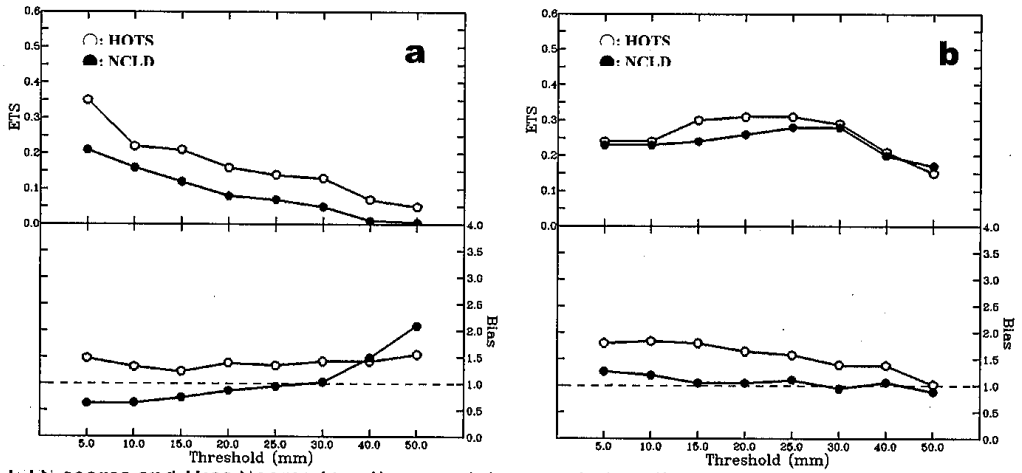

Fig. 2. ETS scores and Bias scores for all precipitation prediction thresholds for the four tropical systems. a) shows results for the 0 to 6-hour forecasts and b) shows results for the 6 to 12-hour forecasts. Open circles (labeled HOTS) are the diabatic forecast results; the filled circles (labeled NCLD) are the cold-started model runs. On the bias plots the Bias =1 line is dashed.

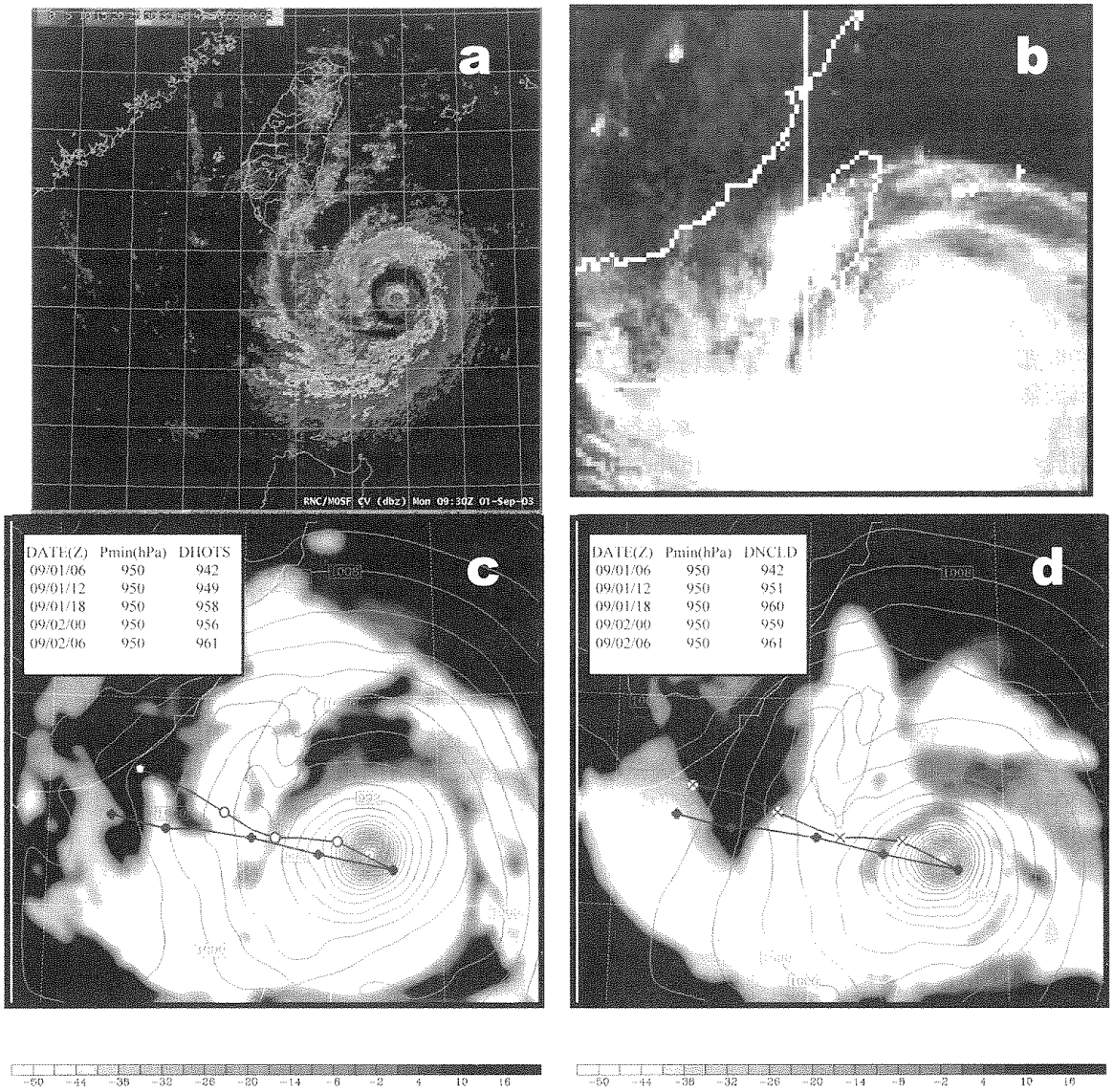

Fig. 3. (a) Radar reflectivity from Doppler radars in Taiwan at 0900 UTC 1 September 2003, (b) GOES-9 IR satellite photograph at 0900 UTC 1 September 2003, and the 3-h predicted cloud top temperature from (c) DHOTS, and (d) DNCLD valid at 0900 UTC 1 September. The analysis from the CWB (filled circles) and predicted tracks of Typhoon Dujuan are shown in 6-h intervals in (c) and (d). Distributions of predicted sea-level pressure are also shown with a contour interval of 2-hPa.